Theoretical Prediction of New High-Performance Lead-Free Piezoelectrics

Pio Baettig,[†,‡] Charles F. Schelle,[†] Richard LeSar,[†,§] Umesh V. Waghmare,[||] and Nicola A. Spaldin*[,†]

Materials Department, University of California, Santa Barbara, California 93106-5050, Chemistry Department, University of Fribourg, Pérolles, 1700 Fribourg, Switzerland, Theoretical Division, Los Alamos National Laboratory, Los Alamos, New Mexico 87545, and Theoretical Sciences Unit, J. Nehru Centre for Advanced Scientific Research, Bangalore, 560 064 India

Received November 8, 2004. Revised Manuscript Received January 12, 2005

We predict the occurrence of large ferroelectric polarization and piezoelectricity in the hypothetical perovskite-structure oxides, bismuth aluminate ($BiAlO_3$) and bismuth gallate ($BiGaO_3$), using density functional theory within the local density approximation. We show that $BiGaO_3$ will have a similar structure to $PbTiO_3$, although with much stronger tetragonal distortion and therefore improved ferroelectric properties. Likewise, $BiAlO_3$ shares structural characteristics with antiferrodistortive $PbZrO_3$, but it is also a ferroelectric with large polarization. Therefore, we propose the $Bi(Al,Ga)O_3$ system as a replacement for the widely used piezoelectric material, $Pb(Zr,Ti)O_3$ (PZT), that will avoid the environmental toxicity problems of lead-based compounds. Finally, we show that, in both $BiAlO_3$ and $BiGaO_3$, the large distortions from the prototypical cubic structure are driven by the stereochemical activity of the Bi lone pair.

1. Introduction

The most widely used piezoelectric material today is the substitutional ceramic $PbZr_{1-x}Ti_xO_3$ (PZT); applications include medical ultrasound devices, smart structures in automobiles, and naval sonar and micromachines, to name a few. The market for such devices is huge, estimated to be tens of billions of dollars worldwide for sensors alone.[1] The large piezoelectric response of PZT ($\sim$2700 μC/cm^2 for poled ceramics[2]) results from two factors. First, the stereochemical activity of the 6s^2 lone pair on the lead ion causes large structural distortions from the prototypical cubic perovskite phase, and in turn strong coupling between the electronic and structural degrees of freedom.[3] And second, high sensitivity is caused by the competition between the different structures of the end point compounds $PbTiO_3$ and $PbZrO_3$ at the so-called morphotropic phase boundary in the solid solution.[4] However, PZT poses significant environmental problems because of its high lead content.

Our goal in this work is to identify new, lead-free ferroelectric materials with large polarizations and piezoelectric responses. In particular, we seek materials whose properties match (or surpass) those of $PbTiO_3$ and $PbZrO_3$ so as to identify nontoxic alternatives for PZT without any loss in performance. There has been some progress in this direction. Recent experimental[5,6] and theoretical[7] studies have suggested $BiScO_3$ as a possible replacement for $PbZrO_3$ in PZT. Likewise, solid solutions of $(Bi,La)(Ga_{0.05}Fe_{0.95})O_3$[8,9] and $Bi(Ga,Sc)O_3$[10,11] with $PbTiO_3$ show promising properties. While substitution of $PbZrO_3$ by a Bi-based compound would clearly halve the amount of lead, an entirely lead-free system would be preferable. In this context, some solid solutions based on $BaTiO_3$ are being explored[12] and solid solutions of $AgNbO_3$ with $BaTiO_3$ or $BaZrO_3$ have recently been proposed.[13] A very recent report of large piezoelectric constants in solid solutions of $(K_{0.5}Na_{0.5})NbO_3$ with $LiTiO_3$ is particularly promising.[14]

The avenue that we pursue is the use of bismuth-based materials, which, for a number of reasons, are good alternatives to Pb-based systems. First, Bi-based compounds have similar or larger levels of ion off-centering than Pb-based compounds, driven by the stereochemically active 6s^2 lone pairs on the Bi^{3+} ion.[15,16] This leads to large ferroelectric polarizations; a value of $\sim$90 μC/cm^2 was recently reported

* To whom correspondence should be addressed.
† University of California, Santa Barbara.
‡ University of Fribourg.
§ Los Alamos National Laboratory.
|| J. Nehru Centre for Advanced Scientific Research.

(1) Busch-Vishniac, I. J. *Phys. Today* **1998**, *51*, 28.
(2) Berlincourt, D. A.; Cmolik, C.; Jaffe, H. *Proc. IRE* **1960**, *48*, 220.
(3) Cohen, R. E. *Nature* **1992**, *358*, 136.
(4) Guo, R.; Cross, L. E.; Park, S. E.; Noheda, B.; Cox, D. E.; Shirane, G. *Phys. Rev. Lett.* **2000**, *84*, 5423.
(5) Eitel, R. E.; Randall, C. A.; Shrout, T. R.; Rehrig, P. W.; Hackenberger, W.; Park, S.-E. *Jpn. J. Appl. Phys.* **2001**, *40*, 5999.
(6) Eitel, R. E.; Randall, C. A.; Shrout, T. R.; Park, S.-E. *Jpn. J. Appl. Phys.* **2002**, *41*, 1.
(7) Iniguez, J.; Vanderbilt, D.; Bellaiche, L. *Phys. Rev. B* **2003**, *67*, 224107.
(8) Cheng, J.-R.; Eitel, R.; Cross, L. E. *J. Am. Ceram. Soc.* **2003**, *86*, 2111.
(9) Cheng, J.-R.; Cross, L. E. *J. Appl. Phys.* **2003**, *94*, 5188.
(10) Cheng, J.-R.; Eitel, R.; Li, N.; Cross, L. E. *J. Appl. Phys.* **2003**, *94*, 605.
(11) Zhang, S.; Priya, S.; Shrout, T. R.; Randall, C. A. *J. Appl. Phys.* **2003**, *93*, 2880.
(12) Yilmaz, H.; Trolier-McKinstry, S.; Messing, G. L. *J. Electroceram.* **2003**, *11*, 217.
(13) Grinberg, I.; Rappe, A. M. *Appl. Phys. Lett.* **2004**, *85*, 1760.
(14) Saito, Y.; Takao, H.; Tani, T.; Nonoyama, T.; Takatori, K.; Homma, T.; Nagaya, T.; Nakamura, M. *Nature* **2004**, *432*, 84.
(15) Hill, N. A.; Rabe, K. M. *Phys. Rev. B* **1999**, *59*, 8759.
(16) Seshadri, R.; Hill, N. A. *Chem. Mater.* **2001**, *13*, 2892.

10.1021/cm0480418 CCC: $30.25
Published on Web 02/22/2005

for $BiFeO_3$ thin films[17] and confirmed by first-principles computations.[18] In addition, they have considerably higher transition temperatures to the paraelectric phase, resulting in reduced temperature dependence of the properties under room-temperature operating conditions. Finally, Bi is nontoxic in its oxide forms; indeed, the active ingredient of a popular antacid is bismuth salicylate.

Our first step is to identify candidate Bi-based materials which have similar structures to the PZT end members, $PbTiO_3$ and $PbZrO_3$. The structures of ferroelectric $PbTiO_3$ and antiferrodistortive $PbZrO_3$ can both be viewed as low-symmetry distortions of the cubic perovskite ABO_3 structure, which they adopt above their Curie temperatures. Single crystals of $PbTiO_3$ have a tetragonal ground state with a ferroelectric polarization[19] of 75 $\mu C/cm^2$, a corresponding Curie temperature of 500 °C, and a high piezoelectric response ($e_{33} = 335\ \mu C/cm^2$ and $e_{13} = -98\ \mu C/cm^2$).[20,21] The ferroelectric polarization and tetragonal symmetry result from the relative displacements of the anion and cation cages along one of the Cartesian axes of the cubic unit cell. $PbZrO_3$ is not ferroelectric, but rotations of the oxygen octahedra around the *x* and *y* axis combine with antiferroelectric displacements of the Pb ions to reduce the symmetry to orthorhombic, with a transition to the cubic phase at about 250 °C.[22]

The different behaviors of the two compounds can be explained, at least in part, by the different relative sizes of the ions. In $PbZrO_3$, the large radius of the B cation, and correspondingly large oxygen cage, means that the A site holes are too big for the Pb ions. This drives the rotation of the octahedra. Conversely, the small B cation in $PbTiO_3$ results in smaller A sites and so there is no room for rotations to occur. These relationships are often quantified using the *tolerance factor*, *t*, defined as

$$t = \frac{r_A + r_O}{\sqrt{2}(r_B + r_O)}$$

where r_A, r_B, and r_O are the ionic radii of the A, B, and oxygen ions, respectively.[23] A tolerance factor less than unity suggests rotational instabilities (in $PbZrO_3$ the value is 0.97) and $t > 1$ points instead to ferroelectric distortions (the tolerance factor of $PbTiO_3$ is 1.03).

Here, we focus on bismuth gallate ($BiGaO_3$) and bismuth aluminate ($BiAlO_3$) as possible replacements for $PbZrO_3$ and $PbTiO_3$, respectively. Our choice is motivated by similarities between the tolerances factors of $BiGaO_3$ ($t = 0.97$) and $BiAlO_3$ ($t = 1.01$) and those of $PbZrO_3$ and $PbTiO_3$. This leads us to anticipate similar structural distortions in the end-point compounds and similar behavior in the solid solution. There is almost no experimental information about either material in its pure phase. A 1947 report in the Hungarian journal *Müegyentemi Közlemények*[24] states that $BiAlO_3$ exists in a tetragonal perovskite structure with a doubled unit cell and lattice parameters 7.61 and 7.94 Å, but there is no reference to a synthetic route, nor mention of material properties. There are, to our knowledge, no experimental reports of perovskite $BiGaO_3$, nor any previous theoretical studies of $BiAlO_3$ or $BiGaO_3$.

Additional motivation for our study is provided by the desire to understand ferroelectricity in materials in which the *only* chemical driving force for off-centering is the lone pair on the A-site Bi ion. In most common ferroelectrics the B-site cations contribute strongly to the ferroelectricity, by off-centering to increase the chemical bonding between their valence d orbitals and the surrounding oxygen 2p orbitals (the so-called second-order Jahn Teller (SOJT) effect.[25,26,27]) Here, the empty Al 3d and Ga 4d orbitals are so high-lying in energy that they are unlikely to have a strong chemical interaction with the surrounding oxygens, and so will not be SOJT-active. Similar behavior is expected in the emerging class of "multiferroic" perovskites which have simultaneous ferroelectric and magnetic ordering.[28] In the most well-studied multiferroics, for example, $BiMnO_3$[15,29] and $BiFeO_3$,[17] the magnetic B-site cation is not SOJT-active, and therefore the ferroelectricity is driven entirely by the A-site cation. By replacing the Mn^{3+} or Fe^{3+} in the Bi-based multiferroics with Al^{3+} or Ga^{3+}, we are able to isolate the role of bismuth in ferroelectricity without the additional complication of magnetic behavior.

The remainder of this paper is organized as follows: In section 2 we describe the computational methods used in this work. In section 3 we present our calculated phonon spectra for hypothetical cubic $BiAlO_3$ and $BiGaO_3$, and compare with those of $PbTiO_3$ and $PbZrO_3$. In section 4 we present our calculated ground-state crystal structures of $BiAlO_3$ and $BiGaO_3$, as well as their electrical properties, and show that simple considerations of tolerance factors do not correctly predict the behavior of the ground state. The implications are discussed in section 5.

2. Computational Details

The calculations described in this work were performed using the ABINIT,[30,31] PWSCF,[32] and VASP[33] implementations of density functional theory and density functional linear response. Our ABINIT and PWSCF calculations were carried out using optimized

(17) Wang, J.; Neaton, J. B.; Zheng, H.; Nagarajan, V.; Ogale, S.; Liu, B.; Viehland, D.; Vaithyanathan, V.; Schlom, D.; Waghmare, U. V.; Spaldin, N. A.; Rabe, K. M.; Wuttig, M.; Ramesh, R. *Science* **2003**, *299*, 1719.
(18) Neaton, J. B.; Ederer, C.; Waghmare, U. V.; Spaldin, N. A.; Rabe, K. M. *Phys. Rev. B* **2005**, *71*, 014113.
(19) Gavrilyachenko, V. G.; Spinko, R. I.; Martynen, M. A.; Fesenko, R. G. *Sov. Phys. Solid State* **1970**, *12*, 1203.
(20) Li, Z.; Grimsditch, M.; Foster, C. M.; Chan, S, K. *J. Phys. Chem. Solid* **1996**, *141*, 1433.
(21) Saghi-Szabo, G.; Cohen, R. E.; Krakauer, H. *Phys. Rev. Lett.* **1998**, *80*, 4321.
(22) Fujishita, H.; Hoshino, S. *J. Phys. Soc. Jpn.* **1984**, *53*, 226.
(23) Goldschmidt, V. M. *Naturwissenschaften* **1926**, *14*, 477.
(24) Naray-Szabo, I. *Müegyentemi Közlemények* **1947**, 32.
(25) Halasyamani, P. S.; Poeppelmeier, K. R. *Chem. Mater.* **1998**, *10*, 2753.
(26) Opik, U.; Pryce, M. L. H. *Proc. R. Soc. A* **1957**, *238*, 425.
(27) Bader, R. F. W. *Mol. Phys.* **1960**, *3*, 137.
(28) Hill, N. A. *J. Phys. Chem. B* **2000**, *104*, 6694.
(29) dos Santos, A. M.; Parashar, S.; Raju, A. R.; Zhao, Y. S.; Cheetham, A. K.; Rao, C. N. R. *Solid State Commun.* **2002**, *122*, 49.
(30) "http://www.abinit.org", The ABINIT code is a common project of the Universite Catholique de Louvain, Corning Incorporated, and other contributors.
(31) Gonze, X. et al. *Comput. Mater. Sci.* **2002**, *25*, 478.
(32) Baroni, S.; Dal Corso, A.; de Gironcoli, S.; Giannozzi, P. http://www.pwscf.org.
(33) Kresse, G.; Furthmüller, J. *Phys. Rev. B* **1996**, *54*, 11169.

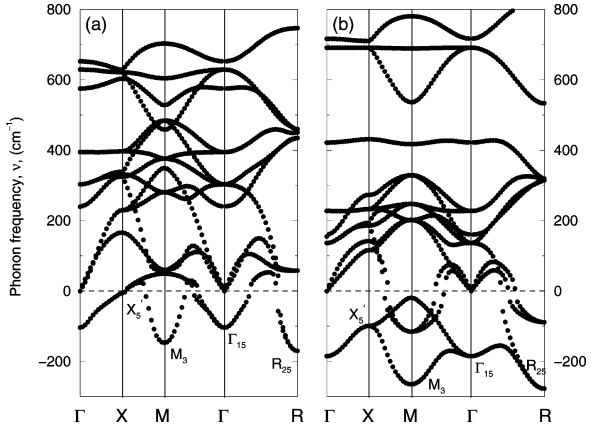

Figure 1. Phonon dispersions for (a) cubic $BiAlO_3$ and (b) cubic $BiGaO_3$ along the high-symmetry lines of the Brillouin zone. Symmetry labels are provided for all high-symmetry modes that correspond to lattice instabilities.

pseudopotentials, with semicore d states included in the valence for Bi and Ga. We used an energy cutoff of 120 Ry, and a $6 \times 6 \times 6$ Monkhorst-Pack grid[34] in calculations for single (five atom) perovskite unit cells, with the appropriate reduction for supercells. Structures were optimized using the Broyden, Fletcher, Goldfarb, Shanno (BFGS)-based method[35] and their local stability was confirmed through calculation of phonons at high-symmetry points (Γ and *R*) using DFT linear response. The exchange-correlation was described using the Perdew−Zunger parametrization[36] of the Ceperley-Alder local density approximation (LDA) exchange-correlation potential.[37] Our VASP[33] calculations used the PAW implementation[38] with the supplied potentials Bi_d, Ga_d, Al, and O. We used a cutoff energy of 550 eV for geometry optimization and of 450 eV for total energy and Berry-phase calculations. In all cases we chose a $6 \times 6 \times 6$ *k*-point grid containing the Γ point, which was checked against calculations with a Monkhorst-Pack[34] grid. Berry phase calculations[39−41] for determining the spontaneous electric polarization were carried out using VASP, employing a $6 \times 6 \times 10$ *k*-point mesh.

3. Structural Instabilities

A well-established method for predicting low-symmetry distortions in cubic perovskites is to first obtain the equilibrium lattice constant for the ideal cubic phase, and then to evaluate the spectrum of vibrational modes (phonons) at that lattice constant.[42] Phonons with imaginary frequencies correspond to structural instabilities of the cubic phase and indicate a lower symmetry ground state. A so-called "Γ-point" instability, in which the atoms in each unit cell move in the same manner, is indicative of ferroelectricity. Other modes lead to different low-symmetry structures. The calculated phonon band structure of $BiAlO_3$, at our calculated LDA lattice constant of 3.75 Å, and that of $BiGaO_3$, at our calculated LDA lattice constant of 3.83 Å, are shown in Figure 1. Imaginary frequency phonons are plotted on the negative *y*-axis. The symmetry labels for the most unstable high-symmetry modes are marked on the plot. Note that both compounds have instabilities throughout the entire Brillouin zone, with those in $BiGaO_3$ being considerably stronger than those in $BiAlO_3$. Compared with earlier calculations for $BaTiO_3$, $PbTiO_3$, and $PbZrO_3$, both phonon spectra are rather similar to that of antiferrodistortive $PbZrO_3$.[42] The unstable ferroelectric Γ_{15} mode corresponds to motion of the bismuth ion opposite to motion of all the other ions in the unit cell. The unstable modes at M and R are both antiferroelectric rotations of the oxygen octahedra, whereas that at X shows opposing motion of the bismuth and equatorial oxygen atoms.

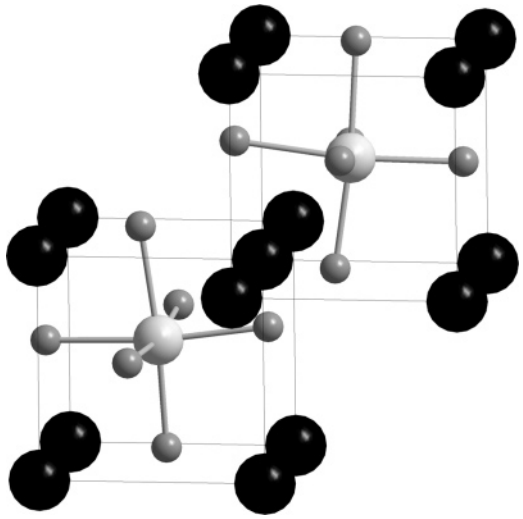

Figure 2. Predicted structure of $BiAlO_3$. The Bi ions are in black, the Al ions in light gray, and the O ions in dark gray.

4. Ground State Crystal Structure and Properties

Next, we calculate the crystallographic ground states of $BiAlO_3$ and $BiGaO_3$. To ensure that we sample all likely structures, and to avoid problems with local structural minima and excessive computer time, we adopt the approach of freezing in pairs of unstable phonon modes and then optimizing the structure within the resulting symmetry using the standard method of minimizing the Hellmann−Feynman forces on the ions. We repeat many of our structural optimizations with the ABINIT, PWSCF, and VASP codes so as to cross check our results. We use the following combinations of modes for our starting structures (the subscripts indicate the direction of the distortion): X_5' alone (*Pmma* symmetry); M_3 alone (*P*4/*mbm* symmetry); $\Gamma_{[100]}$ (*P*4*mm* symmetry); $\Gamma_{[110]}$ (*Cm* symmetry); $\Gamma_{[111]}$ (*R*3*m* symmetry); $\Gamma_{[100]} + M_3$ (*P*4*bm* symmetry); $\Gamma_{[100]} + X_5'$ (*Pmm*2 symmetry); $\Gamma_{[100]} + R_{25}$ (*P*1 symmetry); R_{25} alone ($R\bar{3}c$ symmetry); $\Gamma_{[111]} + R_{25}$ (*R*3*c* symmetry); $\Gamma_{[111]} + R_{25}$ (*R*3 symmetry).

4.1. $BiAlO_3$ Structure. Our calculated ground-state structure for $BiAlO_3$ has *R*3*c* symmetry and is reached from the cubic structure by freezing in two distortions: the antiferrodistortive rotations of adjacent oxygen octahedra in opposite directions along the [111] direction (the R_{25} mode), plus the off-center displacements of the anion cage relative to the cations along [111] (the Γ mode along [111]) as shown in Figure 2. In this respect it *combines* the antiferrodistortive

(34) Monkhorst, H. J.; Pack, J. D. *Phys. Rev. B* **1976**, *13*, 5188.
(35) Shanno, D. F.; Phua, K.-H. *Math. Program.* **1978**, *14*, 149.
(36) Perdew, J. A.; Zunger, A. *Phys. Rev. B* **1981**, *23*, 5048.
(37) Ceperley, D. M.; Alder, B. J. *Phys. Rev. Lett.* **1980**, *45*, 566.
(38) Kresse, G.; Joubert, D. *Phys. Rev. B* **1999**, *59*, 1758.
(39) King-Smith, R. D.; Vanderbilt, D. *Phys. Rev. B* **1993**, *47*, R1651.
(40) King-Smith, R. D.; Vanderbilt, D. *Phys. Rev. B* **1994**, *49*, 5828.
(41) Resta, R. *Rev. Mod. Phys.* **1994**, *66*, 899.
(42) Ghosez, P.; Cockayne, E.; Waghmare, U. V.; Rabe, K. M. *Phys. Rev. B* **1999**, *60*, 836.

behavior of $PbZrO_3$ with the ferroelectric behavior of $PbTiO_3$, although the ferroelectric polarization lies along the diagonal rather than the edge of the primitive unit cell. The *R*3*c* structure is 250 meV per formula unit lower in energy than the cubic structure, whereas the energy gains obtained by optimization from the Γ [111] mode alone (*R*3*m* symmetry) or the R_{25} mode alone ($R\bar{3}c$ symmetry) are only 200 and 180 meV, respectively. The structure is close to ideal rhombohedral (the rhombohedral angle is 59.78°, compared to the ideal value of 60°), and the calculated lattice constant is 3.84 Å, slightly larger than that of the cubic phase. We obtain an approximate Curie temperature, T_c, of 800 K, by equating the energy difference between the ground state and the centrosymmetric $R\bar{3}c$ state to kT_c.

Notice that our calculated rhombohedral structure is inconsistent with our expectations based on analysis of the tolerance factor, which predicted the absence of rotational distortions. To confirm that our results are not an artifact of the local density approximation, which is known to systematically underestimate lattice constants in comparison with experiment, we repeated our total energy calculations for the lowest energy *R*3*c* and *R*3*m* structures over a range of enlarged cell sizes up to a 2% increase over the LDA lattice constant. In all cases the *R*3*c* remained lowest in energy. Our calculated structure is also inconsistent with the early experimental report (ref 43) of a tetragonal perovskite structure, with unit cell doubling in each direction. The reported lattice parameters were 7.61 and 7.94 Å, which corresponds to a *c*/*a* ratio of 1.04. These parameters are consistent with a structure obtained by freezing in both the R-point instability and the *tetragonal* Γ point instability, a combination which we find to be higher in energy than the ground state by ~85 meV. We hope that our calculations will stimulate more experimental work in this area.

4.2. $BiGaO_3$ Structure. Next, we determine the ground-state structure of $BiGaO_3$ by calculating the energies of structures optimized in the same symmetries as those listed above. In this case we obtain a tetragonal ground state, reached by freezing in the Γ point instability along the [100] direction. The tetragonality is unusually large; the *a* lattice constant is 3.64 Å, and the *c*/*a* ratio is 1.3. Indeed, the distortions are so strong that $BiGaO_3$ is effectively a layered material, with alternating (100) planes of Bi−O and Ga−O. Both the Bi and the Ga are strongly off-centered, with alternating Ga−O distances of 1.81 and 2.86 Å along the [100] direction, and Bi−O distances of 2.30 and 3.74 Å. Again, the computed structure is not predicted by consideration of the tolerance factor, which suggests antiferrodistortive rotations for the ground state. See Figure 3.

4.3. Calculated Electronic Properties. We find that the ferroelectric properties of both ground-state structures are very favorable. For $BiAlO_3$, we calculate a change in ferroelectric polarization from the centrosymmetric structure of 75.6 $\mu C/cm^2$ along the [111] direction, and a piezoelectric stress constant[44] in the same direction, $\partial P_{[111]}/\partial strain_{[111]}$, of 320 ± 10 $\mu C/cm^2$. (The clamped ion contribution is −57.0 ± 0.5 $\mu C/cm^2$.) The corresponding numbers for $BiGaO_3$ are

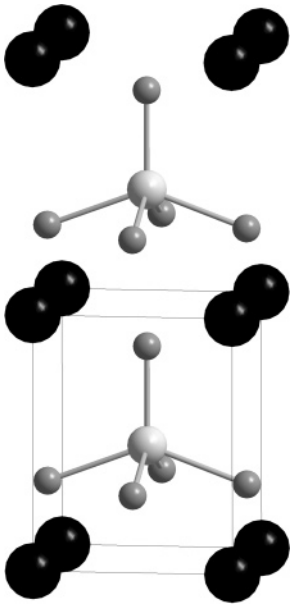

Figure 3. Predicted structure of $BiGaO_3$. The Bi ions are in black, the Ga ions in light gray, and the O ions in dark gray.

151.9 $\mu C/cm^2$ along [100] for the polarization and −165.4 ± 1.2 $\mu C/cm^2$ for the e_{33} piezoelectric constant (change in polarization along [100] when the strain is applied along [100]); the clamped ion value is 56.5 ± 0.1 $\mu C/cm^2$. The polarization value of 151.9 $\mu C/cm^2$ is, to our knowledge, the largest value ever predicted for a perovskite ferroelectric and reflects the large displacements of the Bi and Ga ions from their centrosymmetric positions. In particular, it is larger than the calculated value for $PbTiO_3$.[21]

5. Discussion

Our calculations suggest that $BiAlO_3$ and $BiGaO_3$ will likely be excellent ferroelectric materials, with among the largest polarizations known, high Curie temperatures and significant piezoelectric responses. In addition, since the structures of the two end-point compounds are distinctly different, we anticipate that a $Bi(Ga,Al)O_3$ solid solution could show even higher response properties in the region of the phase boundary between the two ground-state structures. From a technical standpoint, our results indicate that ferroelectrics in which the B-site cation is chemically inert, and the displacements are driven entirely by the activity on the A-site, can indeed have excellent ferroelectric and piezoelectric properties. This augurs well for the ferroelectric response of multiferroic materials, in which the magnetic B-site cation is prohibited from undergoing an off-centering second-order Jahn−Teller distortion.

The large polarization and piezoelectric response are a result of the stereochemical activity of the Bi lone pairs, which causes large displacements of the Bi ions from their positions in the centrosymmetric phase. This is illustrated in Figure 4, where we show our calculated electron localiza-

(43) Naray-Szabo, I. *Müegyentemi Közlemények* **1947**, 32.

(44) Note that the piezoelectric stress coefficients, e_{ij}, give the polarization arising from a small strain at zero electric field, $P_{induced,i} = e_{ij}\eta_j$, or the stress induced by an applied field at zero strain, $\sigma_j = e_{ij}E_i$. They are related to the piezoelectric strain coefficients, d_{ij}, by the elastic constants.

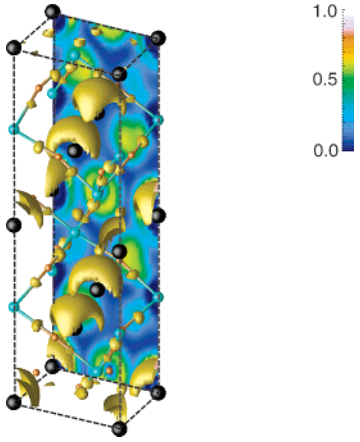

Figure 4. Calculated electron localization function for the ground-state *R*3*c* structure of $BiAlO_3$. The Bi ions are in black, the Al ions in blue, and the O ions red.

tion function[45] (ELF) for $BiAlO_3$ at a value of 0.65, obtained using the STUTTGART TB-LMTO-ASA-code.[46] The polar [111] axis is oriented vertically (the Bi−Al−Bi−Al−Bi ordering can be seen clearly along the front right edge of the cell); a slice through the ELF is shown on the back panel. The localized lone pairs on the Bi ions can be clearly seen as the yellow lobe-shaped regions of high electron localization.

The activity of the Bi ion in driving the structural distortions is confirmed by our calculations of Born effective charges (*Z**'s), which are anomalously large on the Bi ions. *Z** is defined as the derivative of the polarization with respect to the atomic position at zero macroscopic electric field, or equivalently as the linear-order coefficient between the electric field and the force that the field exerts on an ion at zero displacement. A large *Z** indicates that even a small electric field arising from atomic displacements yields a large force, thus favoring the tendency toward a polarized ground state. Previous work on ferroelectric perovskites[47−50] has clearly shown that the Born effective charges on the ions that displace during the phase transition are "anomalous", in that they are far larger than (often almost double) the nominal ionic charges.

Table 1 shows our calculated *Z** values for $BiAlO_3$ and $BiGaO_3$, together with literature values for $PbTiO_3$ and $BaTiO_3$. For $BaTiO_3$, anomalous charges exist on the Ti ion (almost double the 4+ formal charge) and on the oxygen in the direction of the Ti−O bond, $O_{||}$ (nearly three times the 2− formal charge). The *Z**s on the Ba^{2+} ion and on the O^{2-} ions in the direction perpendicular to the Ti−O bond ($O_\perp$) are very close to the formal charge values. This is consistent with the ferroelectric stabilization resulting from charge transfer between the Ti and $O_{||}$ ions, whereas the Ba^{2+} ions, which do not have any states available for hybridization with the oxygens, do not change their charge state during the phase transition. In $BiAlO_3$ and $BiGaO_3$ the situation is exactly opposite that of $BaTiO_3$. The Bi ion shows a strongly anomalous *Z**, more than double its formal 3+ charge, which is consistent with the activity of the Bi $6s^2$ lone pair in stabilizing the ferroelectric distortion. The $O_\perp$, which mixes with the Bi during the ferroelectric phase transition, is also markedly anomalous. The Al^{3+} and Ga^{3+} ions and the $O_{||}$, however, have *Z**s very close to their formal values, indicating that they do not rehybridize through the ferroelectric phase transition. Interestingly, $PbTiO_3$ combines the B-site and $O_{||}$ anomalies of $BaTiO_3$ with (to a lesser extent) the A-site and $O_\perp$ anomalies of $BiAlO_3$ and $BiGaO_3$.

Table 1. Born Effective Charges for the ABO_3 Compounds: $BiAlO_3$ (This Work), $BiGaO_3$ (This Work), $BaTiO_3$,[47] and $PbTiO_3$[51] [a]

	Z_A*	Z_B*	$Z_{O\|\|}$*	$Z_{O\perp}$*
$BiAlO_3$	6.22	2.84	−2.34	−3.38
$BiGaO_3$	6.29	3.11	−2.58	−3.40
$BaTiO_3$	2.75	7.16	−5.69	−2.11
$PbTiO_3$	3.87	7.07	−5.71	−2.51

[a] $Z_{O||}$* is the born effective charge on the oxygen atom in the direction of the B−O bond, and $Z_{O\perp}$* is the effective charge in the perpendicular direction.

Finally, we point out that the behavior of $BiAlO_3$ is quite distinct from that of $PbTiO_3$, and $BiGaO_3$ is distinct from $PbZrO_3$. Therefore, our initial consideration of similarity in tolerance factors and cation electronic structure was clearly too simplistic to correctly predict the ground-state crystal structures; these are also strongly influenced by the chemistry of the perovskite. Woodward has pointed out[52] that the rhombohedral tiltings of the oxygen octahedra that lead to *R*3*c* or $R\bar{3}c$ structures are more favorable in perovskites with higher valent A-site cations because these rotations optimize Coulomb interactions with the oxygens, which are enhanced for more highly charged cations. This is consistent with our prediction of an *R*3*c* ground state for $BiAlO_3$. However, we do not yet have a simple chemical explanation for the strongly ferroelectric, tetragonal structure of $BiGaO_3$.

Acknowledgment. This work was supported by the National Science Foundation's Chemical Bonding Centers program, Grant No. CHE-0434567. P.B. and N.A.S. thank the Petroleum Research Fund of the American Chemical Society for their support of this work, under Grant No. 39440-AC5M. C.S. acknowledges financial support from the IGERT (Award No. DGE-9987618) and GK-12 LEAPS programs of the National Science Foundation. This work made use of MRL Central Facilities supported by the National Science Foundation under Award No. DMR00-80034. The work of R. LeSar was performed under the auspices of the United States Department of Energy (U.S. DOE under Contract W-7405-ENG-36) and was supported by the Division of Materials Science of the Office of Basic Energy Sciences of the Office of Science of the U.S. DOE. We thank Professor Ram Seshadri for help with the generation of Figure 4.

CM0480418

(45) Silvi, B.; Savin, A. *Nature* **1994**, *371*, 683.
(46) Andersen, O. K. *Phys. Rev. B* **1975**, *12*, 3060.
(47) Zhong, W.; King-Smith, R. D.; Vanderbilt, D. *Phys. Rev. Lett.* **1994**, *73*, 1861.
(48) Posternak, M.; Resta, R.; Baldereschi, A. *Phys. Rev. B* **1994**, *50*, 8911.
(49) Ghosez, P.; Gonze, X.; Michenaud, J.-P. *Ferroelectrics* **1994**, *153*, 91.
(50) Ghosez, P.; Michenaud, J.-P.; Gonze, X. *Phys. Rev. B* **1998**, *58*, 6224.
(51) Waghmare, U. V.; Rabe, K. M. *Phys. Rev. B* **1997**, *55*, 6161.
(52) Woodward, P. M. *Acta Crystallogr. B* **1997**, *53*, 44.